



Uncovering the dominant scatterer in graphene sheets on SiO₂

Jyoti Katoch,^{1,2} J.-H. Chen,³ Ryuichi Tsuchikawa,^{1,2} C. W. Smith,^{1,2} E. R. Mucciolo,¹ and Masa Ishigami^{1,2}

¹*Department of Physics, University of Central Florida, Orlando, Florida 32816-2385, USA*

²*Nanoscience Technology Center, University of Central Florida, Orlando, Florida 32816-2385, USA*

³*Department of Physics, University of Maryland, College Park, Maryland 20742, USA*

(Received 21 May 2010; revised manuscript received 9 July 2010; published 27 August 2010)

We have measured the impact of atomic hydrogen adsorption on the electronic transport properties of graphene sheets as a function of hydrogen coverage and initial, pre-hydrogenation field-effect mobility. Our results are compatible with hydrogen adsorbates inducing intervalley mixing by exerting a short-range scattering potential. The saturation coverages for different devices are found to be proportional to their initial mobility, indicating that the number of native scatterers is proportional to the saturation coverage of hydrogen. By extrapolating this proportionality, we show that the field-effect mobility can reach 1.5×10^4 cm²/V s in the absence of the hydrogen-adsorbing sites. This affinity to hydrogen is the signature of the most dominant type of native scatterers in graphene-based field-effect transistors on SiO₂.

DOI: [10.1103/PhysRevB.82.081417](https://doi.org/10.1103/PhysRevB.82.081417)

PACS number(s): 68.43.-h, 81.05.ue

Freely suspended graphene sheets display high-field-effect mobility, reaching 2×10^5 cm²/V s.^{1,2} High-mobilities allows for a wider utilization of graphene sheets in testing relativistic quantum mechanics, exploring two-dimensional physics, and creating new electronic, optoelectronic, and spintronic device technologies.³⁻⁵ Yet, suspended graphene sheets are fragile and impractical for most experiments and applications. Substrate-bound graphene sheets are easier to handle but possess low-carrier mobilities, which can even vary by an order of magnitude from sample to sample. Poor and unpredictable transport properties reduce the utility of substrate-bound graphene sheets for both fundamental and applied sciences. Therefore, understanding the impact of substrates is crucial for graphene science and technology.

Charged impurities,^{6,7} ripples,⁸ and resonant scatterers⁹⁻¹² have been considered for modeling the transport property of graphene field-effect transistors (FETs). Previous experimental studies have explored the impact of charged impurities¹³ and resonant scatterers¹⁴⁻¹⁷ by using adsorbed impurities or creating vacancies on graphene sheets. Yet, these studies revealed only the impact of adsorbates or vacancies and did not shed information on the nature of the native scatterers already present in the samples. Furthermore, experiments using different dielectric environments have provided contradictory results on the role and importance of charged impurities.^{18,19} Thus, there are no conclusive experimental results revealing the nature of the native scatterers that limit the transport properties of graphene on SiO₂.

We have measured the impact of low-energy atomic hydrogen on the transport properties of graphene as a function of coverage and the initial field-effect mobility. Our transport and Raman spectroscopy measurements show that hydrogen exerts a short-range scattering potential which introduces intervalley scattering. Hydrogen transfers a small but finite amount of charge, as indicated by the gate-dependent transport measurements. The resistivity added by hydrogen remains proportional to the number of adsorbed hydrogen and, therefore, adheres to Matthiessen's rule even at the highest coverage. This shows that adsorbed hydrogen remains rather dilute and does not interfere with other pre-existing scatter-

ing mechanisms. The added resistivity at high-carrier densities varies approximately as n^δ , where n is the carrier density and $\delta \approx -1.5$. Importantly, the saturation coverage of atomic hydrogen is found to be proportional to the inverse initial mobility and, therefore, to the number of pre-existing scattering sites. Finally, our results show that the reactivity to atomic hydrogen is a characteristic manifestation of the most dominant scatterer in graphene sheets on SiO₂.

The graphene FETs in our measurements are prepared using the conventional method.²⁰ Transport properties are measured using the four-probe method.²¹ The initial, pre-hydrogenation mobility ranged from 1900 to 8300 cm²/V s for different graphene devices. Each device is hydrogenated at constant temperature between 11–20 K.²² We use a commercial atomic hydrogen cracker, EFM H from Omicron GmbH, which utilizes a tungsten capillary heated to 2500 K by an electron beam. The cracker also generates high-energy ions which are steered away from graphene using an electric deflector. The dosage rate of atomic hydrogen²³ is maintained constant throughout the measurements using a variable leak valve. The total dosage or accumulated areal dose density can be very different from the actual hydrogen coverage depending on the sticking coefficient. Transport properties are measured at increasing dosages.

Figure 1 shows the impact of atomic hydrogen adsorption on the conductivity of graphene sheets. The changes induced by hydrogen adsorption saturate above a certain dosage. These changes are: (i) a shift in the gate voltage at which the conductivity is minimal (V_{\min}), (ii) an increase in the intensity of the D peak in the Raman spectra, (iii) a monotonic decrease in the conductivity minimum, and (iv) an additional gate-dependent resistivity which varies as $|V_g - V_{\min}|^\delta$, where $\delta \approx -1.5$ at large $|V_g - V_{\min}|$. The gate dependence of the conductivity becomes superlinear at high-dosage levels as a result of this exponent. Below, we discuss each change in more detail.

A finite charge is donated to graphene by the adsorbed hydrogen, as indicated by the shift of V_{\min} upon hydrogenation. The observed sign of the charge transfer from atomic hydrogen to carbon is consistent with a previous

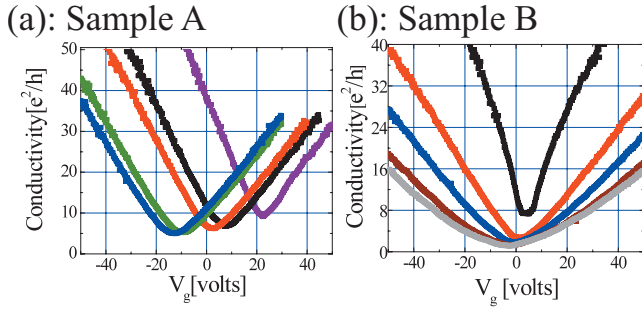


FIG. 1. (Color) (a), (b) Impact of atomic hydrogen on the transport properties of graphene sheets (samples A and B) for increasing areal dosage density. Sample A was measured at 12 K and B at 20 K, respectively. The areal densities, the number of impinging hydrogen (which may not be necessarily adsorbed on graphene), are (a) purple: clean (zero), black: $1 \times 10^{15}/\text{cm}^2$, red: $1.6 \times 10^{15}/\text{cm}^2$, green: $4 \times 10^{15}/\text{cm}^2$, blue: $5.4 \times 10^{15}/\text{cm}^2$, and (b) black: clean (zero), red: $1.4 \times 10^{14}/\text{cm}^2$, blue: $2.8 \times 10^{14}/\text{cm}^2$, brown: $5.6 \times 10^{14}/\text{cm}^2$, and silver: $8.5 \times 10^{14}/\text{cm}^2$.

experiment²⁴ and theoretical calculations^{25,26} but different from hydrogenation studies using atomic hydrogen derived from a hydrogen plasma.^{16,17} It is not possible to determine the amount of charge transferred per adsorbed hydrogen directly from our experiment, as the sticking coefficient of hydrogen on graphene is unknown. Previous experiments^{16,17,24} do not agree on the amount of charge transfer from hydrogen. Theoretical studies show 0.076 to 0.161 e (Ref. 26 or 0.16 to 0.25 e (Ref. 25) donated per hydrogen (e denotes the electron charge), depending on the degree of allowed lattice relaxation²⁶ or the position of hydrogen.²⁵ Below, these calculated values are used to estimate the saturation coverage of hydrogen.

Raman spectroscopy and the impact of atomic hydrogen on the minimum conductivity reveal that atomic hydrogen introduces intervalley scattering and, therefore, exerts a short-range scattering potential.²⁷ Figure 2(a) shows Raman spectra acquired at room temperature in air both before hydrogen dosing and after achieving saturation at low-temperature. The intensity of the D peak in the Raman spectrum is larger upon adsorbing hydrogen. The relative intensity of the D peak to the G peak, I_D/I_G , which can be used to estimate the adsorbed hydrogen density,^{28–30} is 0.0034 ± 0.0021 and 0.0182 ± 0.0056 before and after hydrogen adsorption, respectively.³¹ The small values observed for

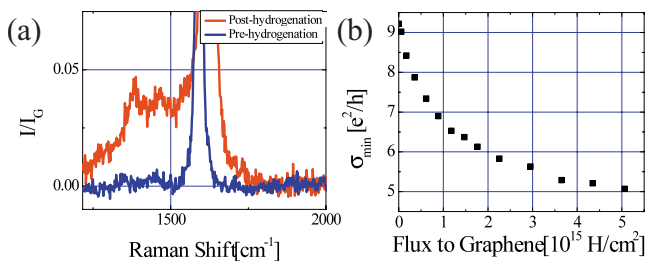


FIG. 2. (Color online) (a) Raman spectra acquired for sample A before and after hydrogenation. The observed intensity has been normalized to the peak height of the G-band. (b) Minimum conductivity as a function of increasing dosage in sample A.

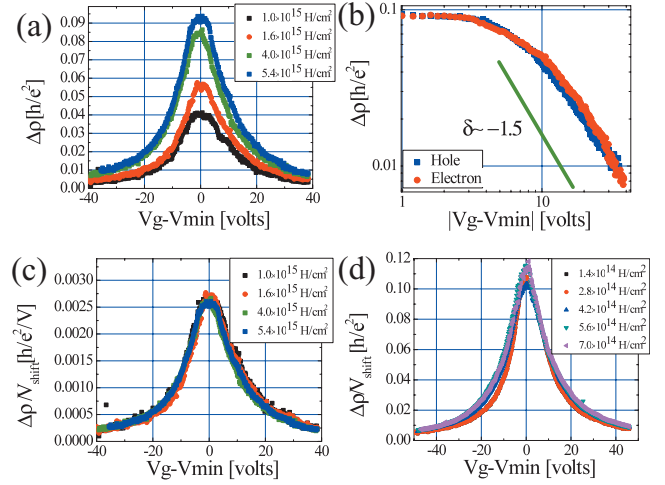


FIG. 3. (Color) (a) Resistivity added by hydrogen as a function of $V_g - V_{\min}$ at different areal dosage density. (b) Gate dependence of the added resistivity as a function of $V_g - V_{\min}$ at the areal dosage density of $5.4 \times 10^{15} \text{ H}/\text{cm}^2$. The green line indicates the slope for an exponent of -1.5 . (c) Added resistivity as a function of $V_g - V_{\min}$ at different areal dosage normalized to V_{shift} . [(a)-(c) for sample A] (d) Same as in (c) but for sample B.

this D-G ratio even at saturation are likely due to the small desorption barrier for hydrogen, as discussed below. Figure 2(b) shows that the minimum conductivity decreases monotonically as a function of hydrogen dosage. The minimum conductivity at saturation ranges from 0.52 to $5.1e^2/h$ for different devices. Since long-range scatterers have been found to vary the minimum conductivity nonmonotonically and not below $4e^2/h$,^{6,13} our transport measurements are also consistent with hydrogen exerting a short-range scattering potential.

Figure 3(a) shows the added resistivity due to atomic hydrogen at different dosage levels as a function of $V_g - V_{\min}$. The impact of atomic hydrogen is nearly electron-hole symmetric and the added resistivity varies approximately as $|V_g - V_{\min}|^{-1.5}$ at large $|V_g - V_{\min}|$ for all samples, as shown in Fig. 3(b). The resistivity exponent differs from the -1 value expected for Coulomb impurities^{6,13} and the electron-hole symmetry is consistent with a resonant scatterer positioned very close to the Fermi level (i.e., a midgap resonant state).³² The observed exponent also agrees with calculated exponents for resonant scatterers with a finite on-site amplitude³³ as well as for Gaussian-correlated scatterers.^{34,35} As shown in Fig. 3(c), we find that the curves of added resistivity versus gate voltage for successive dosage levels collapse on top of each other when divided by the induced shift in V_{\min} , V_{shift} , indicating that the added resistivity at different dosage levels is proportional to V_{shift} . Therefore, the number of adsorbed hydrogen atoms is directly proportional to V_{shift} . For long-range scatterers such as potassium adsorbates,¹³ V_{shift} does not vary linearly with the number of adsorbates. Such nonlinearity has been attributed to incomplete screening of the potential imposed by potassium on graphene.⁶ Therefore, we conclude that the excess charge of adsorbed atomic hydrogen is effectively screened by graphene. All samples we have measured show a similar behavior (for instance, see Fig. 3(d) for

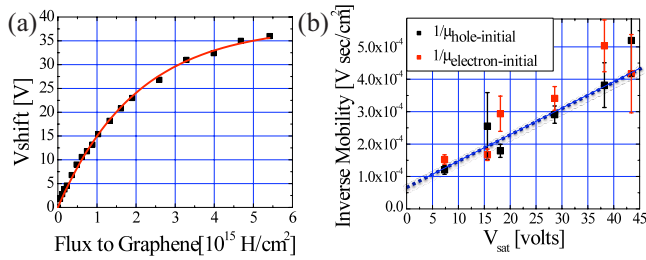


FIG. 4. (Color online) (a) V_{shift} as a function of the increasing areal dosage density for sample A. (b) Initial maximum electron and hole mobility as a function of the saturation voltage shift, V_{sat} , for different samples.

sample B). Deviations from the observed normalization by V_{shift} are found only at low-dosages and can be attributed to uncertainty in determining V_{min} at low-dosage. The observed normalization also shows that the scattering cross-section of hydrogen does not vary appreciably even at higher dosage levels and that hydrogen does not modify other scattering mechanisms. Therefore, the added resistivity by hydrogen follows Matthiessen's rule, $R_{\text{total}} = R_{\text{adsorbates}} + R_{\text{substrate}} + R_{\text{graphene}}$, where $R_{\text{adsorbates}}$ and $R_{\text{substrate}}$ are due to scattering by adsorbates and the substrate, respectively, and R_{graphene} is the intrinsic resistance of the graphene sheet.

Figure 4(a) shows V_{shift} , which is proportional to the number of adsorbed hydrogen, as a function of the accumulated hydrogen dosage. The behavior is well described by a saturating exponential function, with a saturation voltage denoted V_{sat} . A wide range of V_{sat} is observed for different samples, from 7.34 to 43.4 V. The maximum shift of 43.4 V implies that the observed maximum coverage of hydrogen is 0.012 assuming the predicted charge transfer²⁶ of $0.076e$ per adsorbed hydrogen. We find no correlation between experimental temperatures and saturation voltages. Figure 4(b) shows that the saturation coverage for different samples is inversely proportional to their initial maximum electron and hole field-effect mobility.³⁶ Since the inverse mobility is proportional to the number of scatterers, our data show that the number of native scatterers is proportional to the number of possible adsorption sites for hydrogen. By extrapolation to the limit where these sites are absent, we obtain a mobility of $(1.5 \pm 0.3) \times 10^4 \text{ cm}^2/\text{V s}$, as determined by a linear fit. This extrapolated mobility value is still an order-of-magnitude lower than the field-effect mobility measured for suspended graphene sheets,^{1,2} showing that there are still other, less important, scatterers reducing the mobility of graphene on SiO_2 . Interestingly, the extrapolated value is similar to the maximum mobility observed on SiO_2 in previous studies^{37,38} suggesting that the reactivity to hydrogen is the signature of the most dominant type of native scatterers for all graphene devices on SiO_2 .

V_{shift} induced by the adsorbed hydrogen is reduced as the temperature is raised, as shown in Fig. 5. The value of V_{shift} remains constant when warmed samples are again cooled, indicating that the observed reduction in V_{shift} is due to the desorption of hydrogen. This temperature dependence indicates that the desorption energy of adsorbed hydrogen on graphene is much smaller than the previously reported values

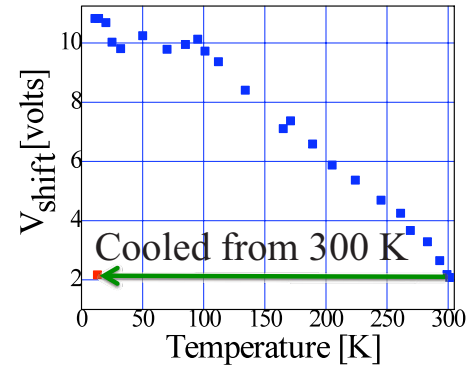


FIG. 5. (Color online) V_{shift} at increasing temperature for sample C after reaching saturation coverage by atomic hydrogen at 11 K. Data acquired at a warming rate of 0.45 to 6 K/min. Red point indicates V_{shift} when the warmed hydrogenated device is cooled down again from 300 K.

of approximately 1 eV on graphite.³⁹ A small desorption energy explains the small D peak observed in the Raman spectra of the hydrogen-dosed samples acquired at room temperature and suggests that atomic hydrogen is not forming a fully relaxed covalent bond to carbon. Furthermore, we also know that the maximum thermal energy of impinging atomic hydrogen barely exceeds the barrier of 0.21 eV calculated for the attachment of atomic hydrogen to planar graphite.⁴⁰ Therefore, atomic hydrogen is binding only to unusual, chemically-activated sites, which do not relax to a full sp^3 configuration upon adsorbing hydrogen.

It is possible that the reactivity of graphene sheets is enhanced by adding curvature or changing the Fermi level. Wrinkles^{41,42} and ripples⁸ can perturb the sp^2 bonds, generating chemically-activated sites for hydrogen. Charge puddles⁶ may also increase the reactivity of graphene sheets. However, the data presented in this Rapid Communication cannot determine the sites with affinity to atomic hydrogen in graphene on SiO_2 . Atomically-resolved microscopy on hydrogenated graphene devices can reveal the exact mechanism for the enhancement of the reactivity, correlated with the most dominant scatterer in graphene on SiO_2 . These studies are being presently carried out.

In conclusion, we used atomic hydrogen to probe the nature of native scatterers in graphene. Hydrogen exerts short-range scattering potential in graphene, as indicated by Raman spectroscopy and the impact on the minimum conductivity. Charge is transferred from hydrogen to carbon and the Coulomb potential created by the induced charge on hydrogen is effectively screened by carriers in graphene. The adherence of the added resistivity to Matthiessen's rule also shows that: (i) adsorbates do not influence the resistivity caused by other factors (such as lattice defects, phonons, etc.) and (ii) the number of adsorbed hydrogen, n_H , is proportional to V_{shift} . Finally, the number of hydrogen adsorption sites is found to correspond to the number of native scatterers; in the absence of these scatterers, the carrier mobility of graphene sheets will reach $1.5 \times 10^4 \text{ cm}^2/\text{V s}$. The scatterers uncovered in this study dominate the transport properties of graphene-based FETs on SiO_2 and the affinity to atomic hydrogen is the hallmark of these scatterers. Our

results provide an important insight into the nature of the scatterers which limit mobility of graphene sheets on substrates.

This work is based upon research supported by the National Science Foundation under Grant No. 0955625. M.I.

thanks Enrique del Barco and Simranjeet Singh for collaboration in developing the graphene device fabrication procedure at UCF and providing access to photolithography and electron-beam evaporator facilities. EM thanks Rodrigo Capaz, Vitor Pereira, and Nuno Peres for fruitful discussions.

- ¹K. I. Bolotin *et al.*, *Solid State Commun.* **146**, 351 (2008).
- ²K. I. Bolotin *et al.*, *Phys. Rev. Lett.* **101**, 096802 (2008).
- ³A. H. Castro Neto *et al.*, *Rev. Mod. Phys.* **81**, 109 (2009).
- ⁴A. K. Geim, *Science* **324**, 1530 (2009).
- ⁵A. K. Geim and K. S. Novoselov, *Nature Mater.* **6**, 183 (2007).
- ⁶S. Adam *et al.*, *Proc. Natl. Acad. Sci. U.S.A.* **104**, 18392 (2007).
- ⁷T. Ando, *J. Phys. Soc. Jpn.* **75**, 074716 (2006).
- ⁸M. I. Katsnelson and A. K. Geim, *Philos. Trans. R. Soc. London, Ser. A* **366**, 195 (2008).
- ⁹P. M. Ostrovsky, I. V. Gornyi, and A. D. Mirlin, *Phys. Rev. B* **74**, 235443 (2006).
- ¹⁰T. Stauber, N. M. R. Peres, and F. Guinea, *Phys. Rev. B* **76**, 205423 (2007).
- ¹¹M. Titov *et al.*, *Phys. Rev. Lett.* **104**, 076802 (2010).
- ¹²T. O. Wehling, M. I. Katsnelson, and A. I. Lichtenstein, *Phys. Rev. B* **80**, 085428 (2009).
- ¹³J. H. Chen *et al.*, *Nat. Phys.* **4**, 377 (2008).
- ¹⁴J. H. Chen *et al.*, *Phys. Rev. Lett.* **102**, 236805 (2009).
- ¹⁵A. Bostwick *et al.*, *Phys. Rev. Lett.* **103**, 056404 (2009).
- ¹⁶D. C. Elias *et al.*, *Science* **323**, 610 (2009).
- ¹⁷Z. H. Ni *et al.*, *arXiv:1003.0202.v2* (unpublished).
- ¹⁸L. A. Ponomarenko *et al.*, *Phys. Rev. Lett.* **102**, 206603 (2009).
- ¹⁹C. Jang *et al.*, *Phys. Rev. Lett.* **101**, 146805 (2008).
- ²⁰Graphene is obtained from Kish graphite by mechanical exfoliation (Ref. 43) on 280 nm SiO₂ over doped Si, which is used as the back gate. Raman spectroscopy is used to confirm that the samples are single layer graphene.⁴⁴ Au/Cr electrodes, defined by electron-beam lithography, contact the graphene sheets. The devices are annealed in H₂/Ar at 300 °C for 1 hour to remove resist residues.⁴⁵ Each device is annealed in ultrahigh vacuum at 490 K for longer than 8 hours to eliminate any residual adsorbates prior to hydrogen dosing experiments.
- ²¹The voltage probes were placed on graphene areas measuring (length × width) 5.0 × 6.4 μm² (sample A), 0.74 × 0.31 μm² (sample B), and 7.8 × 8.2 μm² (sample C).
- ²²Dosing is done at a constant temperature, which varied between different devices.
- ²³The dosage rate is estimated from the angular distribution of atomic hydrogen provided by the manufacturer.
- ²⁴S. Ryu *et al.*, *Nano Lett.* **8**, 4597 (2008).
- ²⁵Z. H. Zhu, G. Q. Lu, and F. Y. Wang, *J. Phys. Chem. B* **109**, 7923 (2005).
- ²⁶M. A. Carneiro and R. B. Capaz (private communication).
- ²⁷L. M. Malard *et al.*, *Phys. Rep.* **473**, 51 (2009).
- ²⁸M. M. Lucchese *et al.*, *Carbon* **48**, 1592 (2010).
- ²⁹L. G. Cançado *et al.*, *Appl. Phys. Lett.* **88**, 163106 (2006).
- ³⁰K. Sato *et al.*, *Chem. Phys. Lett.* **427**, 117 (2006).
- ³¹Multiple Lorentzian peaks near 1250, 1350, and 1450 cm⁻¹ were fitted to the experimental data to determine the peak height.
- ³²N. M. R. Peres, F. Guinea, and A. H. C. Neto, *Phys. Rev. B* **73**, 125411 (2006).
- ³³E. R. Mucciolo and N. M. R. Peres (unpublished).
- ³⁴S. Adam, P. W. Brouwer, and S. D. Sarma, *Phys. Rev. B* **79**, 201404 (2009).
- ³⁵Previous calculations^{10,11,46} using resonant scatterers with infinite on-site energy yield a resistivity exponent less or equal to -1.
- ³⁶ $\mu = \frac{1}{c_g} \frac{d\sigma}{dV_g}$ where μ is field-effect mobility and c_g is capacitance per unit area, was used to calculate the gate-dependent mobility.
- ³⁷S. V. Morozov *et al.*, *Phys. Rev. Lett.* **100**, 016602 (2008).
- ³⁸Y. W. Tan *et al.*, *Phys. Rev. Lett.* **99**, 246803 (2007).
- ³⁹T. Zecho *et al.*, *J. Chem. Phys.* **117**, 8486 (2002).
- ⁴⁰J. Kerwin and B. Jackson, *J. Chem. Phys.* **128**, 084702 (2008).
- ⁴¹F. Guinea, B. Horovitz, and P. L. Doussal, *Solid State Commun.* **149**, 1140 (2009).
- ⁴²V. M. Pereira *et al.*, *arXiv:1004.5384.v1* (unpublished).
- ⁴³K. S. Novoselov *et al.*, *Proc. Natl. Acad. Sci. U.S.A.* **102**, 10451 (2005).
- ⁴⁴A. C. Ferrari *et al.*, *Phys. Rev. Lett.* **97**, 187401 (2006).
- ⁴⁵M. Ishigami *et al.*, *Nano Lett.* **7**, 1643 (2007).
- ⁴⁶T. O. Wehling *et al.*, *Phys. Rev. Lett.* **105**, 056802 (2010).